CHAPTER V
RESULTS AND DISCUSSION

In this study, wax deposition experiments were carried out using different system compositions. For monodisperse and polydisperse systems, the percent of each species in the solution was fixed at 4% w/w unless stated otherwise. All trials were conducted using the same operating and experimental conditions. The coldfinger probe was held at 10°C and the bulk fluid temperature was held at 50°C. The stir bar was used to maintain the rotational speed at 340 rpm to ensure similar flow patterns. Each trial was run for 6 hours.

5.1 Monodisperse System Deposition

Figure 5.1 shows that the deposit mass of monodisperse systems increases with its cloud point. This trend is expected because at the same deposition temperature, less soluble materials will come out of solution more because of a higher concentration gradient. Although stearic acid is structurally different from the n-alkane, it follows the trend for n-alkanes as shown in Figure 5.1.

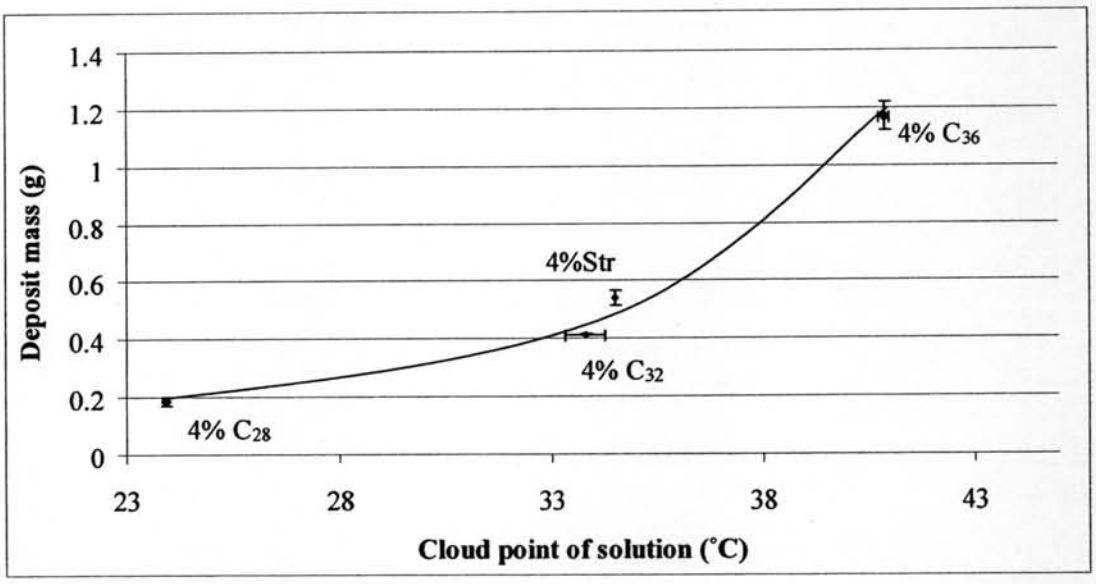

Figure 5.1 Deposit mass of monodisperse systems. *Stearic acid cloud point is from Senra private communication.

Another important quantity to gain a better understanding of wax deposition is the composition of the deposit.

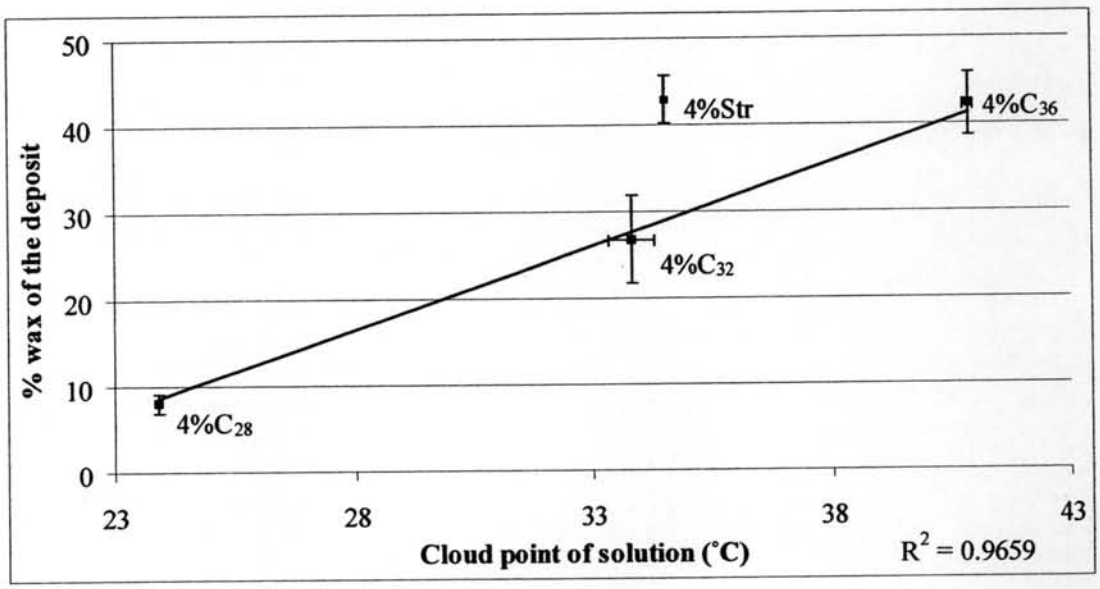

Figure 5.2 % wax of the deposit of monodisperse system

Figure 5.2 shows that the wax composition of the deposit in monodisperse n-alkane systems increases linearly with system cloud point. However, unlike deposit mass, stearic acid does not follow the same trend as the n-alkanes. The deviation of deposit wax fraction can be investigated by using the equations developed in Chapter 4.

$$\frac{d\overline{F}_j(t)}{dt} = \frac{2r_i\left[D_{ejg}\frac{dC_{jg}}{dT}\frac{dT_g}{dr}\right]_i}{\rho_{gel}(r_i^2 - R^2)} \qquad (4.13)$$

Equation 4.13 suggests that the difference in F_{str} and F_{C32} could be caused by differences in $\frac{dT}{dr_i}$, r_i, and D_{ej} between the systems. For the $\frac{dT}{dr_i}$ term, a relationship can be obtained from Equation 4.8 as shown in Equation 5.1.

$$q|_i = -\left.\frac{k_e 2\pi L(T_i - T_a)}{\ln\left(\frac{r_i}{R}\right)}\right|_i = -k_e A|\nabla T|_i = -k_e 2\pi r L \left.\frac{dT}{dr}\right|_i$$

$$\left.\frac{dT}{dr}\right|_i = \frac{T_i - T_a}{r_i \ln\left(\frac{r_i}{R}\right)} \tag{5.1}$$

where

$$T_i = \frac{T_b r_i h \ln\left(\frac{r_i}{R}\right) + k_e T_a}{k_e + r_i h \ln\left(\frac{r_i}{R}\right)} \tag{5.2}$$

and

$$k_e = \frac{[2k_w + k_{oil} + (k_w - k_{oil})F_w]}{[2k_w + k_{oil} - 2(k_w - k_{oil})F_w]} k_{oil} \tag{4.17}$$

Equation 5.2 which is the simplified form of Equation **4.16** is obtained by neglecting the third term of Equation 4.16 as discussed in Chapter 4. Equations 5.1 and 5.2 show that if two depositable materials have different thermal conductivities, $\frac{dT}{dr_i}$ of these two system will not be the same. The effect of k_e on both T_i and $\frac{dT}{dr_i}$ can be seen in Figure 5.3, where k_e is varied between k_{oil} (0.131 W/(m·K)) and k_w (0.25 W/(m·K)).

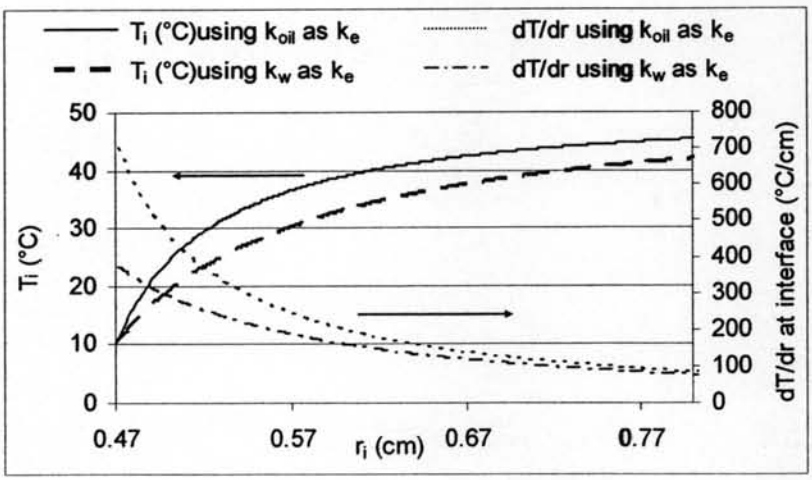

Figure 5.3 Effect of different deposit thermal conductivity on T_i and $\frac{dT}{dr_i}$.

Figure 5.3 shows that a decrease of k_e by 48 percent increases T_i and $\frac{dT}{dr_i}$ by approximately 16 and 27 percent respectively. The thermal conductivity of stearic acid (0.172 W/(m·K)) is lower than wax thermal conductivity (0.25 W/(m·K)) and close to the thermal conductivity of dodecane (0.131 W/(m·K)) (Forsythe 2003; Sharma *et al.*, 2005; Burgdorf *et al.*, 1999). While stearic acid and C_{32} deposits are developing, $\frac{dT}{dr_i}$ of stearic acid will be higher than C_{32} at the same r_i because of a lower thermal conductivity, indicating that the lower thermal conductivity of stearic acid is one reason why stearic acid would have a higher F_j than an n-alkane with a similar cloud point. However, the result in Figure 5.2 shows that F_{Str} is 60% higher than F_{C32}. Therefore, other terms in Equation 4.13 such as the effective diffusivity could play an important role in the increase of F_{Str} from F_{C32}.

5.2 Polydisperse n-Alkane Deposition

Senra (2006) and Guo *et al.* (2004) show that 4%C_{36}-4%C_{32}, 4%C_{32}-4%C_{28} cocrsytallize and that 4%C_{36}-4%C_{28}, 4%C_{32}-4%C_{24} crystallize separately in both dodecane and decane. When n-alkane systems cocrysatllize, Guo *et al.* (2004) suggested that the crystal size will be larger and the crystals will be more compact than the independently crystallized system. From Chapter 4, the difference in crystal aspect ratio will affect the effective diffusivity of wax in the deposit. Therefore, cocrystallized deposits are expected to have different characteristics than the independent crystallized deposit.

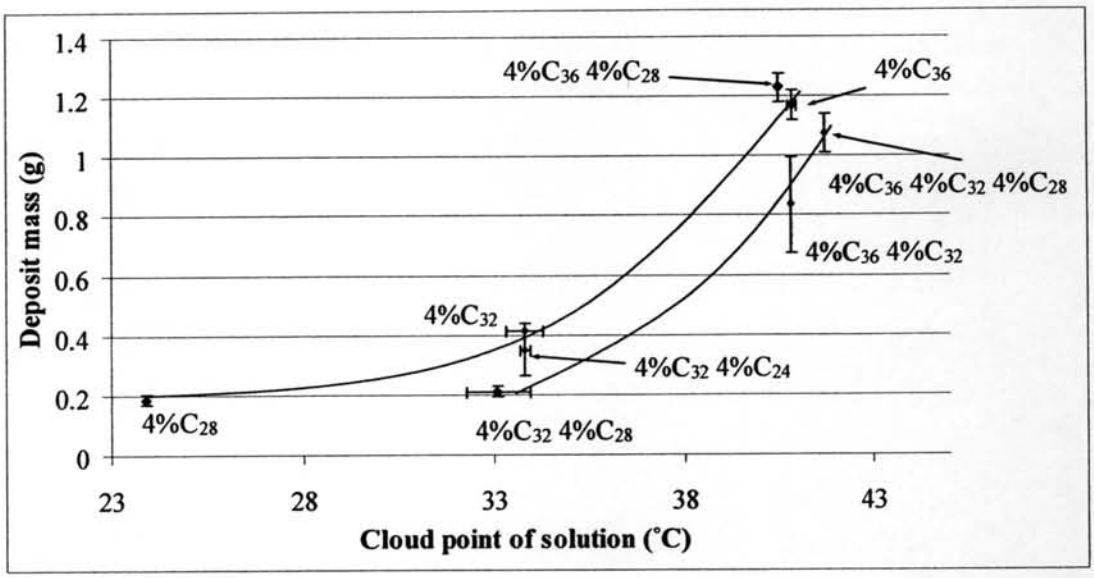

Figure 5.4 Polydisperse system deposit mass as a function of cloud point. *(4%C_{36} 4%C_{32} 4%C_{28}) cloud point is from Senra private communication.

Figure 5.4 shows that the deposit mass of the independently crystallized systems have a similar trend as the monodisperse systems, but the trend is shifted downward, even though these systems have double the wax content. From the polydisperse results, it can be seen that deposit mass is a strong function of system cloud point, but is also significantly impacted by the crystallization mechanism. For cocrystallized systems having relatively the same cloud point as the independently crystallized system, the deposit mass still increases with system cloud point, but the deposit mass is much lower than monodisperse and independently crystallized system. Therefore, cocrystallization inhibits the deposit growth. Cocrystallization could inhibit the deposit growth by modifying the crystal structure of the deposit by increasing deposit crystal aspect ratio. The effect of cocrystallization on deposition inhibition will be discussed again with the deposit composition results and balance equations.

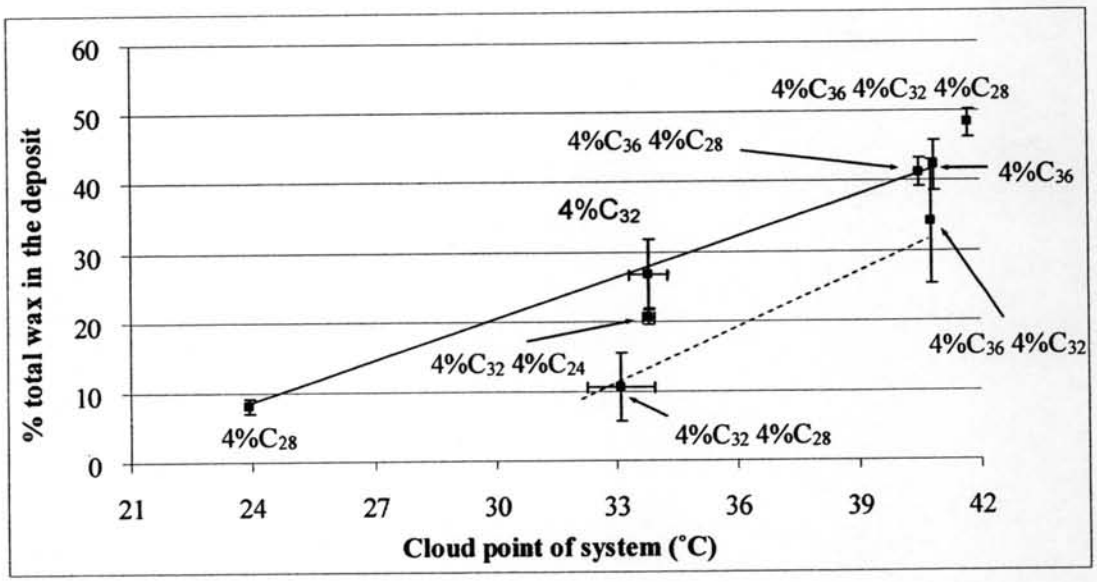

Figure 5.5 % total wax in the deposit.

Another variable of interest besides deposit mass that can be analyzed is deposit composition. Figure 5.5 shows that the F_j of cocrystallized systems increase as their cloud point increase. Figure 5.5 also shows that cocrystallized systems always have lower wax content in their deposit when compared to the monodisperse and independently crystallized polydisperse systems that have approximately the same cloud point.

The interesting issue here is that the cocrystallized deposit has different characteristics than the independently crystallized deposit with the same wax fraction in solution. The net deposition rate of the cocrystallized systems is lower than the independently crystallized systems as shown in Figures 5.4 and 5.5. The two rates which primarily control the net deposition rate could be the deposition rate and the rate of interface crystal structure destroyed due to fluid shear which is the shear reduction term. If the cocrsyatllization deposition rate is higher than the independent crystallization deposition rate, then the shear reduction must be much higher to agree with the experimental results. If cocrystallization deposition rate is lower than the independent crystallization deposition rate, the cocrystallized deposit gel strength could be higher, lower or equal to the independently crystallized deposit gel strength depending on how low the cocrystallization deposition rate is. Thus, the deposit yield stress measurement will help gain a better understanding on what is the major reason

for the difference between the cocrystallized and independently crystallized system kinetics and shear.

From Equations 4.11 and 4.13,

$$D_{ejg} = \frac{D_{jog}}{1+\alpha^2 \overline{F}_w^{\,2}/(1-\overline{F}_w)} \tag{4.11}$$

$$\frac{d\overline{F}_j(t)}{dt} = \frac{2r_i\left[D_{ejg}\frac{dC_{jg}}{dT}\frac{dT_g}{dr}\right]_i}{\rho_{gel}(r_i^2 - R^2)} \tag{4.13}$$

another possible explanation of the lower F_j in the cocrystallized deposit is that the α of the cocrystallized system may be higher than independent crystallized system because when α increases, there will be a greater barrier for depositable material to diffuse into the deposit. In another word, when α increases, D_{ejg} will decrease, causing F_j to increase more slowly.

Table 5.1 can provide insight into how the presence of less and more soluble alkanes impacts deposition. For example, the presence of a more soluble material decreases the ability of the less soluble material to deposit in both cocrystallized and independently crystallized system. However, the degree of this decrease is significantly different for the more soluble material has a greater impact in cocrystallized system. For an independently crystallized binary system, the presence of C_{28} decreases the percent of C_{36} depleted from solution by 15% and C_{24} decreases the percent of C_{32} depleted from solution by 50% when compared to the monodisperse system. However, the percent of C_{36} depleted drops 67% when C_{32} is present and the percent of C_{32} depleted drops 89% when C_{28} is present. Cocrystallized systems also have a lower total percent of depositable material when compared to independently crystallized binary system and monodisperse system.

Table 5.1 Deposit composition observed in various system studied

System	Deposit mass (g) ±< 0.15	% least soluble material in the deposit	% least soluble material depleted from solution	% most soluble material in the deposit	% most soluble material depleted from solution	% total depositable material in the deposit
C_{36}	1.17	42.2 ± 3.6	7.9 ± 0.3			
C_{32}	0.41	26.8 ± 5.1	1.8 ± 0.3			
C_{28}	0.19	8.0 ± 1.1	0.2 ±0.01			
Str	0.54	42.9 ± 2.8	3.7 ± 0.4			
C_{36}-C_{32}	0.82	20.0 ± 5.3	2.6 ± 1.0	14.7 ± 2.5	1.9 ± 0.6	34.8 ± 7.7
C_{32}-C_{28}	0.21	5.0 ± 2.3	0.2 ± 0.1	4.8 ± 1.5	0.2 ± 0.1	9.8 ± 3.8
C_{36}-C_{28}	1.23	35.8 ± 2.1	6.7 ± 0.2	5.4 ± 0.6	1.0 ± 0.1	41.2 ± 0.6
C_{32}-C_{24}	0.41	16.5 ± 1.2	0.9 ± 0.2	4.1 ± 0.1	0.2 ± 0.1	20.5 ± 1.1
C_{36}-C_{32}-C_{28}	1.08	28.4 ± 2.2	4.5 ± 0.6	6.2 ± 0.4	1.0 ± 0.01	48.3 ± 2.0
4%*C_{36}-4%Str	1.39	36.7 ± 1.9	7.8 ± 0.2	6.5 ± 1.0	1.4 ± 0.1	43.1 ± 3.0
4%*C_{36}-2%Str	1.13	41.0 ± 1.6	7.0 ± 0.7	3.3 ± 2.0	1.1 ± 0.5	44.3 ± 3.7
4%*C_{36}-1%Str	1.17	41.4 ± 2.6	7.4 ± 0.6	1.6 ± 0.2	1.2 ± 0.2	43.1 ± 2.8
4%C_{32}-4%*Str	0.72	10.2 ± 0.3	1.2 ± 0.2	8.3 ± 0.5	0.9 ± 0.2	18.5 ± 0.8
4%*C_{32}-2%Str	0.47	10.0 ± 0.9	0.7 ± 0.1	3.0 ± 2.0	0.4 ± 0.3	12.9 ±2.9
4%*C_{32}-1%Str	0.40	10.7 ± 0.1	0.7 ± 0.1	1.1 ± 0.2	0.3 ± 0.03	11.8 ± 0.04

For the more soluble component, the results in Table 5.1 show that the percent of the more soluble material depleted from solution in the cocrystallized

systems remains the same as in the monodisperse cases. However, when the more soluble material independently crystallizes and deposits with the less soluble material, the percent depleted from solution of the more soluble material increases significantly, 5 times for C_{28} when it deposit with C_{36}. Therefore, the less soluble n-alkane enhances the deposition ability of more soluble n-alkane. One possible explanation for this enhancement is that the less soluble n-alkane traps some of the more soluble n-alkane as liquid inside gel structure initially, and the more soluble n-alkane precipitates later when the solubility limit of the more soluble material inside the deposit is reached

For the C_{36}-C_{32}-C_{28} system, Senra (2006) shows that both cocrystallization and independent crystallization occur. Therefore, the results that this ternary system deposit mass follows cocrystallized deposit mass trend and F_j follows independently crystallized F_j trend are possible.

5.3 Effect of Stearic Acid on Wax Deposition

Figure 5.6 shows the percent depleted from solution of C_{36} and C_{32} as a function of % stearic acid present in the system. Figure 5.6 reveals that stearic acid decreases the % depleted of C_{32} by around 50% and by around 10% for C_{36}. Stearic acid also affects n-alkane % depletion nonlinearly, which is consistent with the result of Guo *et al.* (2004) who found that an additive can decrease yield stress up to a certain concentration. Once this concentration is reached, the yield stress begins to increase. A possible explanation of why stearic acid is a greater inhibitor for C_{32} than C_{36} is that stearic acid's cloud point is closer to C_{32} than C_{36}, so it can deposit more in C_{32} system and can modify the crystal structure of the C_{32} system more than the C_{36} system.

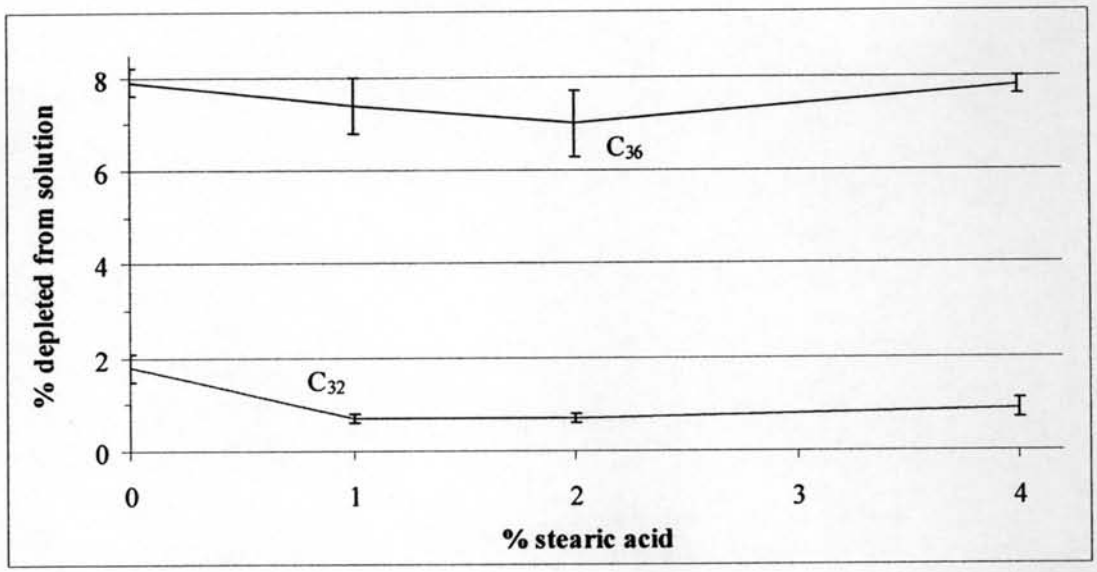

Figure 5.6 Effect of stearic acid on $\%C_{36}$ depleted.